Supporting Information

Stabilization of supramolecular polymer phase at high pressures

N. A. Burger[1,2], A. Mavromanolakis[1], G. Meier[3],

P. Brocorens[4], R. Lazzaroni[4], L. Bouteiller[5], B. Loppinet[1], D. Vlassopoulos[1,2]

1 Foundation for Research & Technology Hellas (FORTH), Institute for Electronic Structure & Laser, Heraklion 70013, Greece

2 University of Crete, Department of Materials Science & Technology, Heraklion 70013, Greece

3 Forschungszentrum Jülich, Institute of Complex Systems (ICS-3), 52425 Jülich, Germany

4 University of Mons, Laboratory for Chemistry of Novel Materials, Materials Research Institute, 7000 Mons, Belgium

5 Sorbonne Université, CNRS, IPCM, Equipe Chimie des Polymères, 75005 Paris, France

EXPERIMENTS

Table S1: Characteristics of tube-filament transition for EHUT in cyclohexane at low pressures.

concentration (g/L)	pressure (bar)	transition temperature (°C)	transition enthalpy (kJ/mol)	technique
10.4	1	52	-	FTIR [1]
4.3	6	49.5	4.3	DSC
0.43	6	47.9	4.0	DSC

DLS data and microrheology:

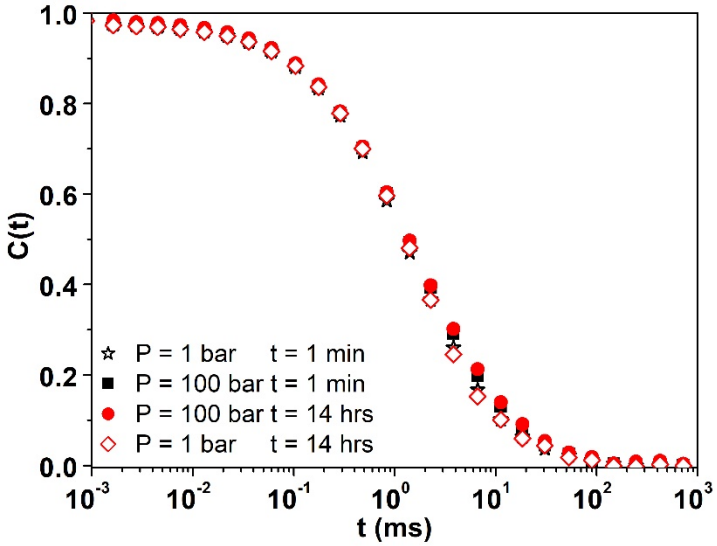

Figure S1: DLS data represented as intermediate scattering functions (ISF) for an EHUT/dodecane solution at concentration 1 g/L with added PMMA hard spheres (at a fraction of 10^{-4} vol%), at different times and pressures, showing identical behavior.

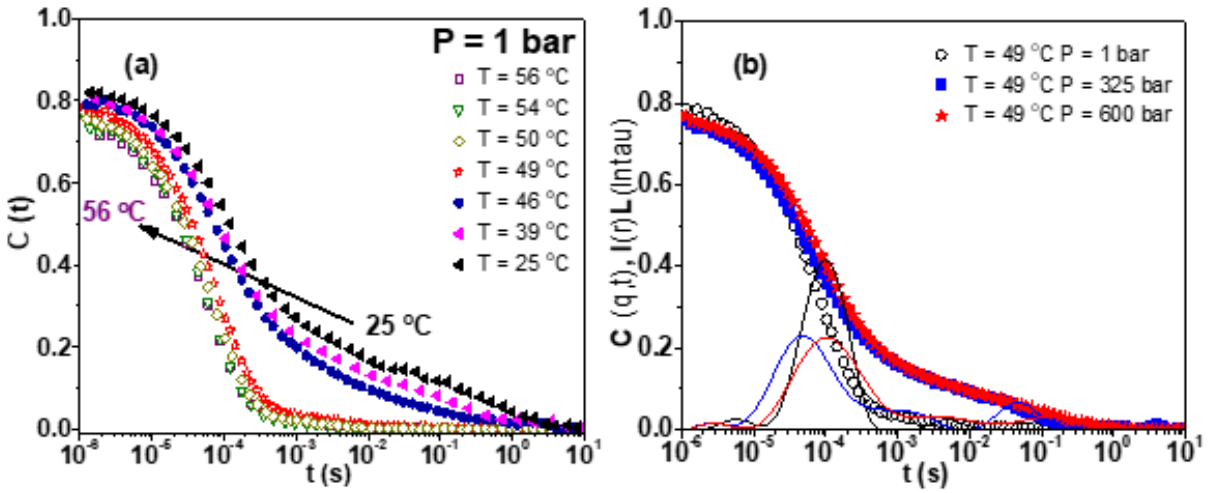

Figure S2: Intermediate scattering functions (ISF); of EHUT/cyclohexane solution at 4 g/L. The open symbols correspond to filaments and the filled to tube structure. (a) Different temperatures at 1 bar. Heating from 25^{O}C (two modes) to 56 ^{O}C (one mode) in the direction of the arrow. (b) At constant temperature (49 ^{O}C) and different pressures (slow mode appears with increase of pressure). The distribution of relaxation times *I(q)L(ln(τ))* is also shown and details of the quantitative analysis are presented in Table S2 below.

The technique of passive microrheology measures the thermal motion of probe particles in a complex fluid.[2] Here we discuss microrheological experiments in the single scattering limit of DLS. The electric field autocorrelation (intermediate scattering) function $C(t)$ is related to the mean square displacement $\langle \Delta r^2 \rangle$ of the colloidal probe particle by $C(t,q)$ or $g_1(t,q) = g_1(0) exp\left(\frac{-q^2\langle \Delta r^2(t)\rangle}{6}\right)$, with the scattering wave vector being $q = \frac{4\pi n}{\lambda} sin\left(\frac{\theta}{2}\right)$. Here, n is the refractive index, λ the wavelength and θ the scattering angle.[3] The generalized Stokes-Einstein-Sutherland equation

$$\widetilde{D}(s) = \frac{k_B T}{6\pi R s \tilde{\eta}(s)} \qquad \text{(S1)}$$

relates the diffusion coefficient $\widetilde{D}(s)$ and the viscosity $\tilde{\eta}(s)$ as functions of the Laplace frequency s, with R the particle radius, $k_B T$ the Boltzmann constant and T the absolute

temperature. Assuming negligible inertial effects, one can deduce the Laplace-transformed complex modulus as

$$\tilde{G}(s) = s\tilde{\eta}(s) = \frac{s}{\pi R}\left[\frac{k_B T}{s^2\langle \Delta r^2(s)\rangle}\right] \quad \text{(S2)}$$

The frequency-dependent linear viscoelastic moduli G'(storage) and G'' (loss) can be obtained from $s = i\,\omega$ and their interrelation $G^* = G' + iG''$ with G^* being the complex modulus. This leads to

$$G^*(\omega) = \frac{k_B T}{\pi R i\omega F\{\langle \Delta r^2(t)\rangle\}} \quad \text{(S3)}$$

where $F\{\langle \Delta r^2(t)\rangle\}$ is the one-side Fourier transform of the mean-square displacement. It has been shown that $\Delta r^2(t)$ can be expanded locally around $t = \frac{1}{\omega}$ by assuming that $\langle \Delta r^2(t)\rangle = \langle \Delta r^2(1/\omega)\rangle (t\omega)^{\alpha(\omega)}$, where the exponent $\alpha(\omega)$ is the local slope of the logarithmic time derivative of $\langle \Delta r^2(t)\rangle$ at $t = \frac{1}{\omega}$. It takes values between 0 (purely elastic material) and 1 (purely viscous). This leads to the following working expressions:[2,4]

$$|G^*(\omega)| = \frac{k_B T}{\pi R\langle \Delta r^2(1/\omega)\rangle \Gamma[1+\alpha(\omega)]} \quad \text{(S4)}$$

$$G'(\omega) = |G^*(\omega)| cos(\pi\alpha(\omega)/2) \quad \text{(S5)}$$

$$G''(\omega) = |G^*(\omega)| sin(\pi\alpha(\omega)/2) \quad \text{(S6)}$$

where $\Gamma[1 + \alpha(\omega)]$ is the gamma function.

Fig. S3 depicts typical microrheological linear viscoelastic spectra at different temperatures and pressures. At atmospheric pressure they compare remarkably well with the respective bulk rheological data.[5] The signatures of tubes and filaments from EHUT are distinct and these results are used in the phase diagram of Fig. 4 of the main text.

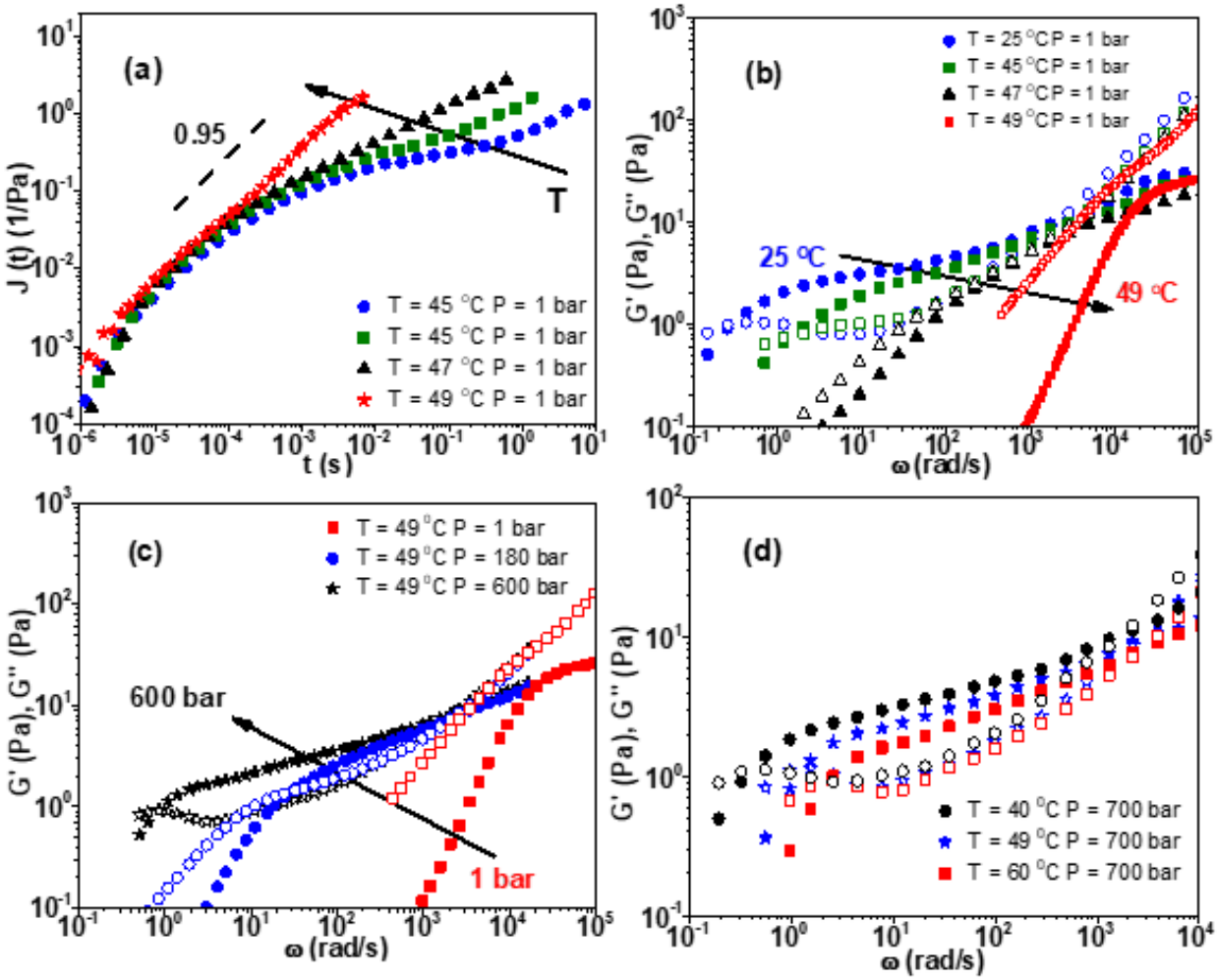

Figure S3. Passive microrheological data. Creep compliance (a) and Frequency dependence (b) of the storage G' (filled symbols) and loss G'' moduli (open symbols) for 4 g/L EHUT / cyclohexane / PMMA solutions in different temperatures and ambient pressure. (c) pressure dependence of the linear vicoelastic spectra at constant temperature of 49^{0}C. (d) Respective data at constant pressure of 700 bar and different temperatures.

Viscosities of solvent and EHUT at two pressure limits corresponding to different phases:

The viscosity of the solvent (cyclohexane) was measured at different temperatures and pressures by passive microrheology with the same conditions (PMMA tracer particles) as for the supramolecular polymers, which are described above and in the main text. The data are shown in Fig.S4 and are consistent with literature data.[6-8] The data are used for the plots of Fig.3 (main text) and Fig.S5 below.

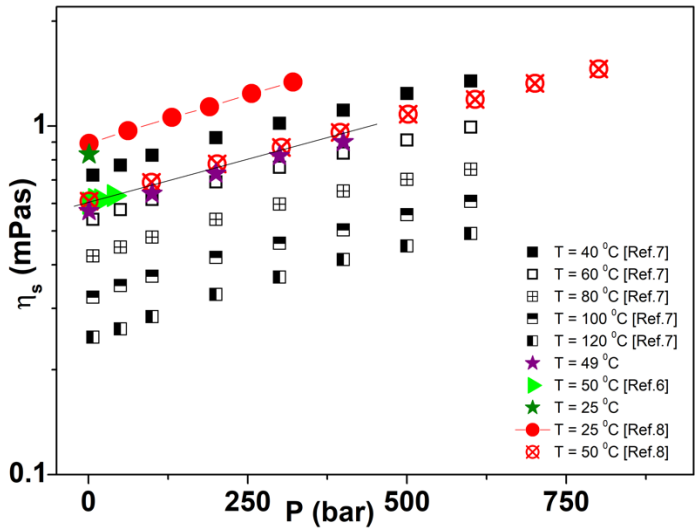

Figure S4: Viscosity of solvent (cyclohexane) as a function of pressure at different temperatures (indicated in the legend) by means of passive microrheology. Data taken from the literature (legend) and measured in this work are included.

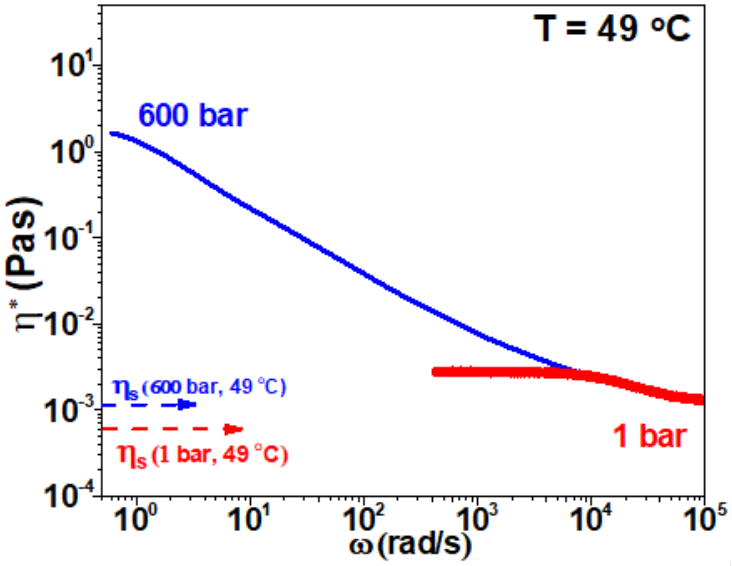

Figure S5: Experimental data of EHUT/cyclohexane solution at 4 g/L. Complex viscosity at 49 ^{O}C. At 1 (red circles) and 600 bar (blue line), measured by passive microrheology. The stars indicate the corresponding solvent viscosity for each pressure at 49 ^{O}C. The relative viscosity (η^* / η_0) changes from ~5 at 1 bar to 1666 at 600 bar.

Analysis of DLS signals:

To determine relaxation times from the $C(q,t)$, we analyzed the latter by means of inverse Laplace transformation (ILT), which was realized using the program CONTIN.[9] In brief, the $C(q,t)$ is described as a superposition of exponentials,

$$\alpha C(q,t) = \int L(ln\tau) \exp\left(-\frac{t}{\tau}\right) dln\tau \qquad \text{(S7)}$$

where α is the amplitude of a relaxation mode and τ its characteristic relaxation time. This provides a continuous spectrum of relaxation times $L(ln\tau)$, with characteristic relaxation modes and their respective relaxation times and amplitudes which, for the data presented (Figs.S2,S6) are listed on Table S2. Note that the broadness of the main fast mode, as characterized by the width at half height, is nearly the same in all cases.

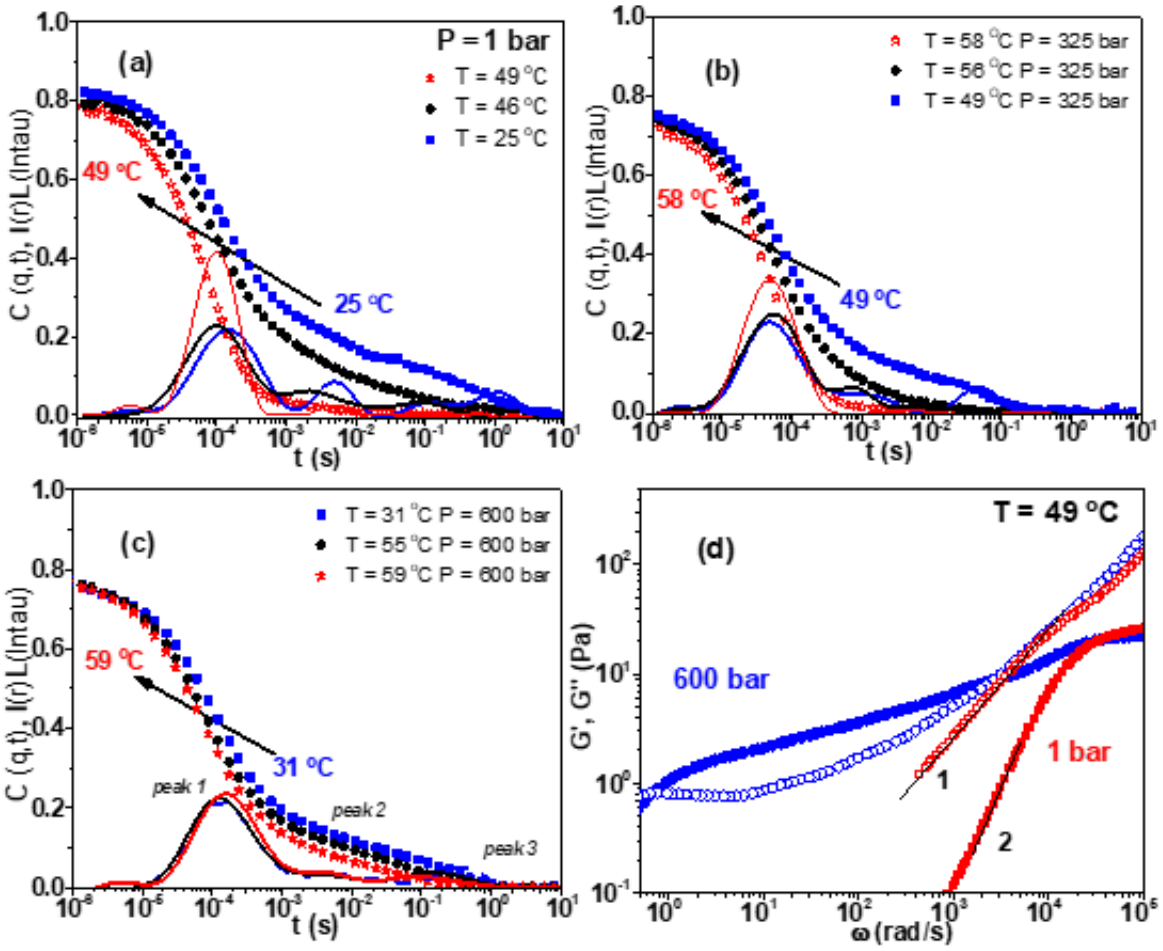

Figure S6: Experimental data for of EHUT/cyclohexane solution at 4 g/L before normalization with the temperature- and volume dependent solvent viscosity. (a) ISF; the open (filled) symbols correspond to filament (tube) structures. Heating from 25^{0}C (two modes) to 49 ^{0}C (one mode) at 1 bar in the direction of the arrow. The distribution of relaxation times *I(q)L(ln(τ))* is also shown. Inset: Average total scattering intensity at different temperatures and pressure of 1 bar ; the red data and arrow indicate the direction of heating, whereas the black data and dashed arrow the cooling direction. (b) ISF and *I(q)L(ln(τ))* for different temperatures upon heating from 49^{0}C to 56^{o}C and eventually 58^{o}C at 325 bar (direction of arrow). (c) Respective ISF and *I(q)L(ln(τ))* data on heating from 31^{0}C to 59^{0}C at 600 bar (direction of arrow). (d) microrheological viscoelastic spectra at 49^{O}C and two different pressures, 1 bar and 600 bar, corresponding to the limit of filaments (red squares) and to tubes (blue circles), respectively. Open (filled) symbols refer to loss modulus G'' (storage modules G').

Table S2: Relaxation times divided by solvent viscosities (τ/η_s) and amplitudes (A) of the ISF modes (with subscripts 1,2,3) of Figure S6 for a 4 g/L EHUT solution in cyclohexane at 1, 325 and 600 bar.

Temperature (^{O}C) (1 bar)	**τ_1/η_0 (1/mPa)**	**A_1**	**τ_2/η_0 (1/mPa)**	**A_2**	**τ_3/η_0 (1/mPa)**	**A_3**
25	1.7×10^{-4}	0.555	5.9×10^{-3}	0.12	1.2	0.1
46	1.7×10^{-4}	0.58	5.6×10^{-3}	0.14	0.135	0.07
49	1.4×10^{-4}	0.74	-	-	-	-
Temperature (^{O}C) (325 bar)	**τ_1/η_0 (1/mPa)**	**A_1**	**τ_2/η_0 (1/mPa)**	**A_2**	**τ_3/η_0 (1/mPa)**	**A_3**
49	1.77×10^{-4}	0.63	2×10^{-3}	0.07	0.074	0.1
56	0.93×10^{-4}	0.66	1.5×10^{-3}	0.09	-	-
58	0.84×10^{-4}	0.71	-	-	-	-
Temperature (^{O}C) (600 bar)	**τ_1/η_0 (1/mPa)**	**A_1**	**τ_2/η_0 (1/mPa)**	**A_2**	**τ_3/η_0 (1/mPa)**	**A_3**
31	0.92×10^{-4}	0.59	6×10^{-3}	0.08	0,198	0.093
55	1.8×10^{-4}	0.67	3.6×10^{-3}	0.058	0.086	0.1
59	1.04×10^{-4}	0.64	3.5×10^{-3}	0.06	0.064	0.074

Analysis of high-frequency loss modulus:

The frequency-dependent loss modulus data for the 4 g/L EHUT solution at 49C and two pressures, 1 bar (filaments) and 600 bar (tubes), are shown in Fig. S7 after the solvent contribution ($\omega\eta_s$) has been subtracted. Motivated by the literature on wormlike micelles,[10] we focus on the high-frequency behavior. In both cases we can observe small albeit unambiguous regimes conforming to power-law scaling with exponents 0.55 in the Rouse-Zimm regime to 0.75 at higher frequencies where internal bending modes dominate for these semiflexible supramolecular polymers. The crossover frequency marking the onset of the bending modes is indicated by arrow in the figure and gives access to the persistence length l_p through

$$\omega_0 = \frac{k_B T}{8\eta_s {l_p}^3} \quad \text{(S8)}$$

yielding nearly the same approximate value of about 40 nm for the two phases. Whereas this number is on the low side (typically values of 100 nm or higher are reported for EHUT solutions[11,12]), we note that the rheological extraction of the persistence length is slightly ambiguous because of the limited range of power-low behavior. Moreover, the above expression S8 suggests the independent relaxation of a Kuhn segment and is approximate. The extraction of characteristic lengths of wormlike micelles from rheometry is a delicate process and there is recent progress,[13] but this is beyond the scope of the present work. We emphasize that the overall data are internally consistent. Finally, the dynamic correlation length or mesh size extracted from the fast (main) relaxation mode of Table S2 by means of the Stokes-Einstein-Sutherland relation amounts to about 30 nm for all cases investigated. In the literature the persistence length is reported to be higher than the mesh size in such systems[12], in agreement with our findings.

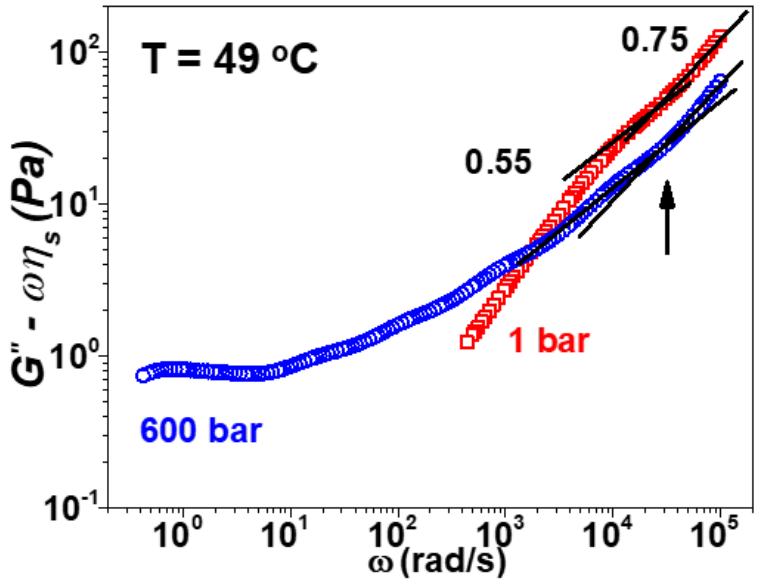

Figure S7: Rescaled data by equation (1). Red squares correspond to 1 bar and blue circles to 600 bar. The dashed lines have a slope of 0.75, filled line 0.55.

SIMULATIONS

Two systems were studied by MD, using the Dreiding force field:[14] tube and a filament of EHUT molecules. The tube was studied with periodic conditions and stronger H-bonding (in Dreiding, the well depth of the hydrogens involved in H-bonding has been set to 10 kcal/mol) to avoid collapse without solvent: a tube of 48 molecules was inserted in a box having lateral dimensions of 100 Å and a longitudinal dimension equal to the tube length, to reproduce a tube of infinite length. Atomic charges were assigned from the Polymer Consistent Force Field (PCFF),[15,16] and long-range interaction were treated by the Ewald method (accuracy 0.001 kcal/mol). The system was submitted to molecular mechanics (MM) energy minimization using the Conjugate gradient algorithm until a convergence criterion of 0.001 kcal per mol.Å was reached. Then a 300 ps molecular dynamics (MD) run was performed at 298 K in NPT conditions with a Berendsen thermostat (decay constant of 0.1 ps), and time steps of 1 fs.

The filament, composed of 32 molecules, was studied without periodic conditions due to the higher flexibility of the assembly.[17] Atomic charges were assigned by PCFF and long-range interactions were treated by an atom-based cutoff of 14 Å with a spline width of 3 Å. The system was submitted to MM energy minimization with the Conjugate gradient algorithm and a convergence criterion of 0.001 kcal per mol.Å. Then a 1500 ps molecular dynamics (MD) run was performed in NVT conditions with time steps of 1 fs. The constructed Connolly surface is depicted in Fig. S8 and the calculated molecular volumes for different probe radii in Fig.S9 (see also main text). The volumes were encompassed by a grid, whose resolution is fine, i.e., with a grid interval of 0.25 Å.

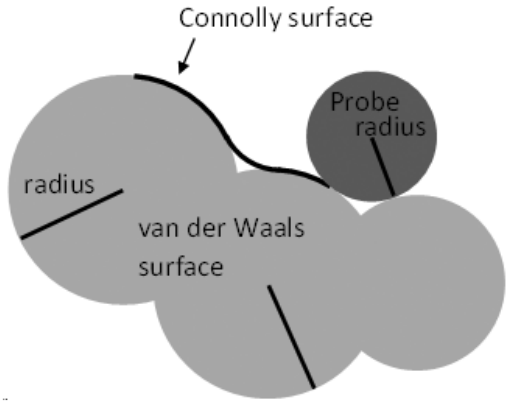

Figure S8: Connolly surface defined by rolling a probe on the molecule; when the probe radius is zero, the molecular surface is called van der Waals surface.

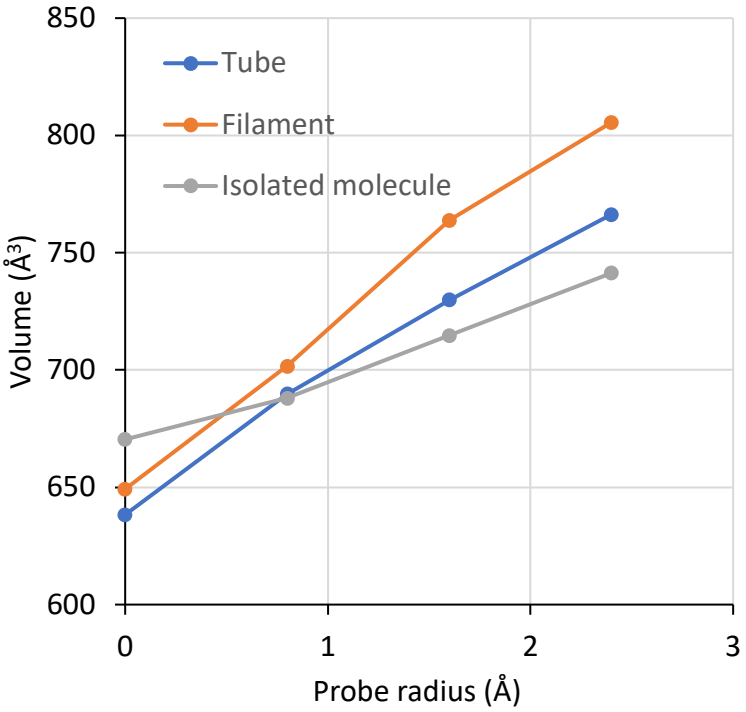

Figure S9: Evolution of the estimated molecular volume for a tube, a filament and an isolated molecule, as a function of the radius of the probe.

References

[1] Bouteiller, L.; Colombani, O.; Lortie, F. ; Terech, P. Thickness transition of a rigid supramolecular polymer. *J. Am. Chem. Soc*. **2005**, *127*, 8893–8898.

[2] Furst, E. M. ; Squires, T. M. *Microrheology*, Oxford University Press, 2017.

[3] Schärtl, W. *Light Scattering from Polymer Solutions and Nanoparticle Dispersions* (Springer Science & Business Media, 2007).

[4] Mason, T. G.E stimating the viscoelastic moduli of complex fluids using the generalized Stokes-Einstein equation, *Rheol. Acta* **2000,** *39*, 371-378.

[5] Louhichi, A. ; Jacob, A. R. ; Boutteiller, L. ; Vlassopoulos, D. Humidity affects the viscoelastic properties of supramolecular living polymers, *J. Rheol*., **2017**, *61*, 1173-1182.

[6] Liu, Z, ; Trusler, J. P. M.; Bi, Q. Viscosities of Liquid Cyclohexane and Decane at Temperatures between (303 and 598) K and Pressures up to 4 MPa Measured in Dual-Capillary Viscometer. *J. Chem. Eng. Data*, **60(8)**, 2363-2370 (2015).

[7] Hernandez-Galvan, M. A. ; Garcia-Sanchez, F.; E. Garcia-Flores, B.; Castro-Arellano, J. Liquid Viscosities of Cyclohexane, Cyclohexane + Tetradecane, and Cyclohexane + Benzene from (313 to 393) K and Pressures Up to 60 MPa. *J. Chem. Eng. Data*, **54(10)**, 2831–2838 (2009).

[8] Tanaka, Y.; Hosokawa, H.; Kubota, H.; Makita, T. Viscosity and Density of Binary Mixtures of Cyclohexane with n-Octane, n-Dodecane, and n-Hexadecane Under High Pressures, *Int. J. Thermophys*., 12, 245-264 (1991).

[9] Provencher, S. W. CONTIN: A general purpose constrained regularization program for inverting noisy linear algebraic and integral equations. *Comput. Phys. Commun*. **1982**, *27*, 229-242.

[10] Willenbacher, N.; Oelschlaeger, C. ; Schopferer, M. ; Fischer, P.; Cardinaux, F.; Scheffold, F. Broad Bandwidth Optical and Mechanical Rheometry ofWormlike Micelle Solutions. *Phys. Rev. Lett*. **2007**, *99*, 068302.

[11] Francisco, K. R.; Dreiss, C. A.; Bouteiller, L.; Sabadini, E. Tuning the Viscoelastic Properties of Bis(urea)-Based Supramolecular Polymer Solutions by Adding Cosolutes. *Langmui*r, **2012**, *28*, 14531-14539.

[12] Knoben, W.; Besseling, N. A. M. ; Cohen Stuart, M. A. Chain Stoppers in Reversible Supramolecular Polymer Solutions Studied by Static and Dynamic Light Scattering and Osmometry. *Macromolecules* **2006**, *39,* 2643-2653

[13] Tan, G.; Zou, W.; Weaver, M.; Larson, R. G. Determining threadlike micelle lengths from rheometry. *J. Rheol*. **2020**, *65*, 59-71.

[14] Mayo, S. L., B. D. Olafson, W. A. Goddard III., "DREIDING: A Generic Force Field for Molecular Simulations", J. Phys. Chem. **94**, 8897-8909 (1990)

[15] Sun, H., "Force field for computation of conformational energies, structures, and vibrational frequencies of aromatic polyesters", J. Comput. Chem. *15*, 752-768 (1994).

[16] Sun, H.,"Ab Initio Calculations and Force Field Development for Computer Simulation of Polysilanes, Macromolecules, *28*, 701-712 (1995).

[17] Alvarenga, B. G.; Raynal, M.; Bouteiller, L.; Sabadini, E. Unexpected Solvent Influence on the Rheology of Supramolecular Polymers. *Macromolecules* **2017**, *50*, 6631-6636.